Supporting Information for

Effects of Surface Roughness on the Electrochemical Reduction of CO_2 over Cu

Kun Jiang,[1,2,3†] Yufeng Huang,[4†] Guosong Zeng,[5] Francesca M. Toma,[2,5]

William A. Goddard, III,[4] and Alexis T. Bell*[2,3,5]

[1]Institute of Fuel Cells, School of Mechanical Engineering, Shanghai Jiao Tong University, Shanghai, 200240

[2]Joint Center for Artificial Photosynthesis, Lawrence Berkeley National Laboratory, Berkeley, California 94720

[3]Department of Chemical and Biomolecular Engineering, University of California, Berkeley, California 94720

[4]Materials Simulation Center and Joint Center for Artificial Photosynthesis, California Institute of Technology, Pasadena, California 91125

[5]Chemical Sciences Division, Lawrence Berkeley National Laboratory, Berkeley, California 94720

[†]These authors contributed equally to this work.

.

Submitted to

ACS Energy Letter

*To whom correspondence should be sent: alexbell@berkeley.edu

Experimental Methods

Electrode Preparation

Cu foil (99.9999% metal basis, Alfa Aesar) was used as the working electrode. The Cu foil was electropolished in 85 wt.% phosphoric acid (99.99% metals basis, Sigma Aldrich) potentiostatically at 3.0 V vs. a graphite rod electrode (99.995% metals basis, Sigma Aldrich) for 300 s, followed by rinsing with Milli-Q water (18.2 MΩ·cm) and drying in a stream of flowing N_2. For plasma pre-treatment, the polished Cu foil was placed in a Plasma-Preen II-973 Reactor (Plasmatic Systems Inc.), evacuated with a mechanical pump to ~5 Torr, and then exposed to a 100-W plasma for 5, 10 or 20 min. Plasma pre-treatment was carried out in N_2, Ar, or O_2 flowing at 1,200 sccm.

Surface Structure Characterization

The morphology of Cu foil electrodes was characterized using a FEI Quanta FEG 250 scanning electron microscope (SEM) operated with an electron beam energy of 15 kV and a spot size of 3.0 nm. Surface topography measurements were performed on a Bruker Dimension Icon atomic force microscopy (AFM) housed in an acoustic and vibration isolation enclosure to minimize the external noise. To determine the surface features, which are comparable to the thickness of an absorbed film of water, the enclosure was purged with dry nitrogen overnight prior to making the measurement. Surface scanning was carried out in the PeakForce mode, using a cantilever with a nominal spring constant of 0.4 N/m (Bruker Scanasyst-Air). The near-surface composition and the chemical state of Cu were determined using a Kratos Axis Ultra DLD X-ray photoelectron spectrometer (XPS). All spectra were acquired using monochromatic Al Kα radiation (15 kV, 15 mA) and a hemispherical electron energy analyzer. The kinetic energy scale of the measured core level spectra was calibrated by setting the C 1s binding energy to 284.6 eV. Raman spectra were collected with a confocal LabRam HR Raman microscope (Horiba) equipped with a 532 nm laser source. Typically, a dispersion grating of 600 g mm^{-1} was used, 128 scans were co-added in order to obtain a good signal-to-noise.

Electrochemical Measurements

All electrochemical experiments were conducted in a gas-tight electrochemical cell machined from polyether ether ketone (PEEK).[1] A glassy carbon plate (Type 2, Alfa Aesar) was used as the

counter electrode, placed parallel to the Cu working electrode and separated by an anion conducting membrane (Selemion AMV AGC Inc.). Gas dispersion frits were incorporated into both electrode chambers to provide ample electrolyte mixing. The exposed geometric surface area of each electrode was 1 cm^2 and the electrolyte volume of each electrode chamber was 1.8 cm^3. Prior to each experiment, both the cell and the counter electrode were sonicated in 20 wt.% nitric acid (diluted from 70% of ACS reagent, Sigma Aldrich) and thoroughly rinsed with Milli-Q water (18.2 MΩ·cm). A leak-free Ag/AgCl electrode (Innovative Instruments Inc.) was used as the reference electrode, all potentials were measured against Ag/AgCl wereand then converted to the RHE scale using the relationship E (vs RHE) = E (vs Ag/AgCl) + 0.197 V + 0.0591×pH, where pH values of electrolytes were determined by an Orion Dual additional pre-reduction step was carried out for 45-min chronoamperometry at -0.6 V in 0.1 M CO_2-saturated $CsHCO_3$.

Electrochemistry was performed with a Biologic VSP-300 potentiostat. Potentiostatic electrochemical impedance spectroscopy (PEIS) and current interrupt (CI) methods were used to determine the uncompensated resistance (R_u) of the electrochemical cell. The potentiostat compensated for 85% of R_u *in-situ*. The roughness factor of Cu foil electrodes was determined relative to the electrochemically polished one, by taking the ratio of their double layer capacitances measured after 1-h electrolysis at -1.0 V vs. RHE, within a 0.1 V potential window centered at the open circuit potential of the system.[2, 3]

CO_2RR Products Quantification

The effluent from the electrochemical cell was analyzed Star Benchtop Meter (Thermo Scientific). A 0.05 M M_2CO_3 (M = Cs or K, 99.995%, Sigma Aldrich) solution prepared using Milli-Q water was used as the electrolyte. Metallic impurities in the as-prepared electrolyte were removed before electrolysis by chelating the solution with Chelex 100 (Na form, Sigma Aldrich). Both electrode chambers were sparged with CO_2 (99.999%, Praxair Inc.) at a rate of 20 sccm for 40 min prior to and throughout CO_2 electrolysis. Prior to CO_2RR measurements on N_2 and O_2 plasma pre-treated Cu foils, an

using an Agilent 7890B gas chromatograph (GC) equipped with a pulsed-discharge helium ionization detector (PDHID). He (99.9999%, Praxair Inc.) was used as the carrier gas. The constituents of the gaseous sample were separated using a Hayesep-Q capillary column (Agilent) connected in series with a packed ShinCarbon ST column (Restek Co.). The signal response of the

PDHID was calibrated by analyzing a series of NIST-traceable standard gas mixtures (Airgas Inc.). The partial current density for a given gas product was calculated as $j_i = x_i \times v \times \frac{n_i F p_0}{RT} \times (electrode\ area)^{-1}$, where x_i is the volume fraction of certain product determined by online GC, v is the flow rate, n_i is the number of electrons required to form product *i*, p_0 = 101.3 kPa, *F* is the Faradaic constant and *R* is the gas constant. The corresponding FE at each potential is calculated using the relationship $FE = j_i / i_{total} \times 100\ \%$. The electrolyte from cathodic chamber was collected after electrolysis and analyzed using a Thermo Scientific UltiMate 3000 liquid chromatography (HPLC) equipped with a refractive index detector (RID). The electrolyte samples were stored in a refrigerated autosampler at 10 °C before analysis to minimize the evaporation of volatile products. The liquid-phase products contained in a 20 µL aliquot were separated using two Aminex HPX 87-H columns (Bio-Rad Inc.) connected in series and a 1 mM sulfuric acid eluent (99.999%, Sigma Aldrich). The column oven was maintained at 60 °C for the duration of the analysis. The signal response of the RID was calibrated by analyzing standard solutions of each product at a concentration of 1, 10, and 50 mM. The CO_2 consumption rate for a given reduction product was calculated as $R_i = N_{C,i} \times j_i \times (n_i \times F)^{-1} \times (electrode\ area)^{-1}$, where $N_{C,i}$ is the carbon chain length of given product, j_i is the partial current density, and the overall CO_2 consumption rate was determined as $R = \sum R_i$.

Computational Details

To simulate plasma roughening of Cu, we used a probabilistic approach in which the Ar^+ cations are assumed to approach the surface vertically from above. The starting structures are the (111) surface of copper. When the Ar^+ contacts the surface, the surface atoms within a cutoff circles (10 Å in radius from the point of impact) are removed to simulate Ar^+ ion bombardment. Each simulated impact removed 140 Cu atoms on average. The structures obtained by this means were relaxed by carrying molecular dynamics simulations using the reactive force field (ReaxFF)[4] approach in a manner similar to that described in Refs.[5-7]. The initial structures were first minimized and relaxed under NVT at 300 K for 1 ps. Then three annealing cycles of 4 ps each with a peak temperature of 1164 K were used to relax the structure further. Finally, the structures were relaxed under NVT at 300 K for another 10 ps. Roughness factors of the final structures were determined in order to relate simulated structures to those obtained experimentally. The

electrochemically polished Cu surface was simulated in the same way but in the absence of Ar^+ bombardment. Instead, the perfect Cu(111) surface was relaxed using the above procedure in order to obtain the electropolished Cu surface. We note that the method used to produce a roughened Cu surface is a computationally efficient and produces a surface roughness roughly equivalent to that achieved by roughening in an Ar plasma.

The CO adsorption energies were predicted on the initial and final Cu surfaces using the neural network developed in Ref. [6]. Briefly, a neural network was fitted on CO adsorption energies calculated from DFT. Using the piecewise cosine functions as symmetry functions,[8] the uncertainty of the model is within 0.12 eV from the DFT values.

Supporting Figures

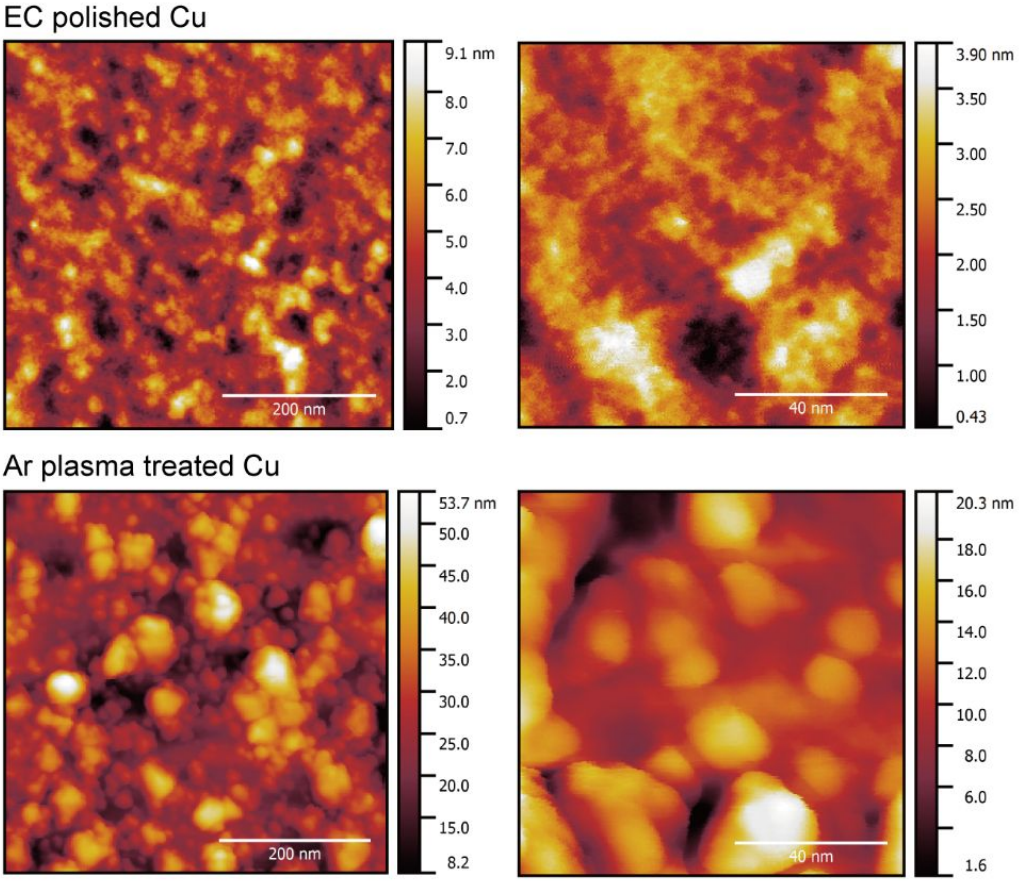

Figure S1. AFM images of electrochemcially polished Cu foil and that after 10-min Ar plasma pre-treatment, scanning area of 500 nm x 500 nm for left panels and 100 nm x 100 nm for right panels.

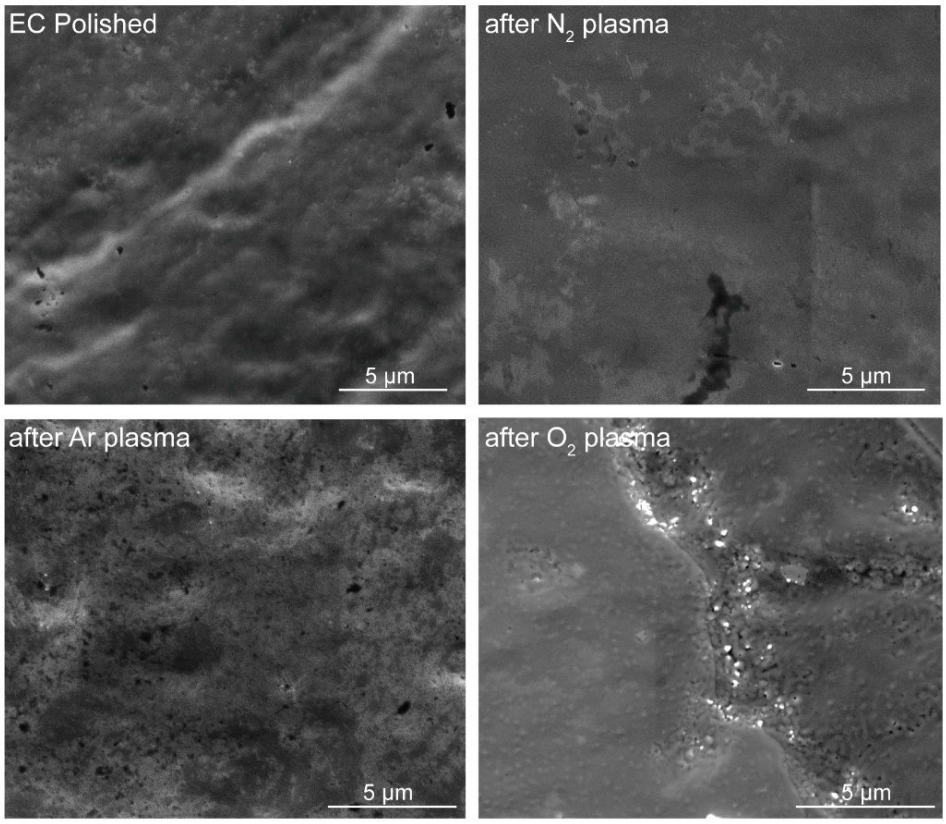

Figure S2. SEM images of Cu foils after 10-min plasma pre-treatments under different atmosphere.

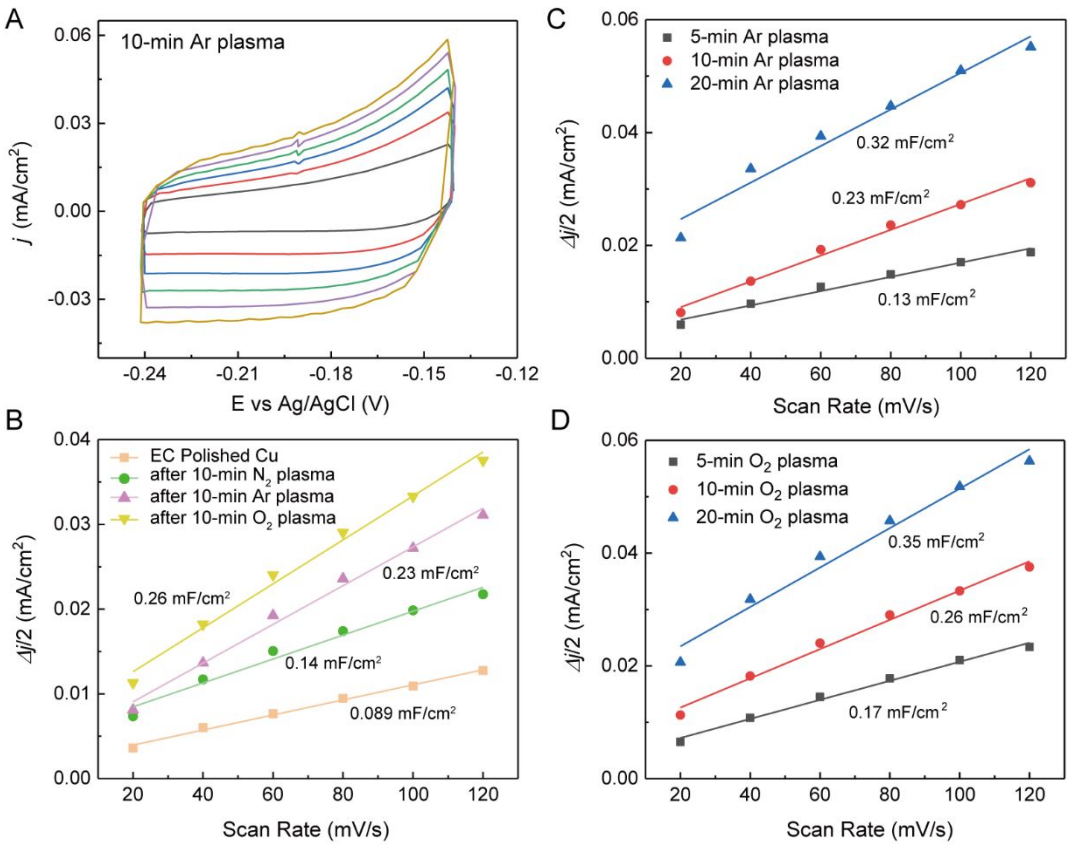

Figure S3. (A) Representative cyclic voltammetry in the double layer potential range at a series of increasing scan rates from 20, 40, 60, 80, 100 to 120 mV s^{-1}, over post-electrolysis Cu foil electrode with 10-min Ar plasma pretreatment. (B-D) Electrochemical active surface area (ECSA) determination by measuring the relevant double layer capacitances and referenced to the electrochemically polished Cu foil.

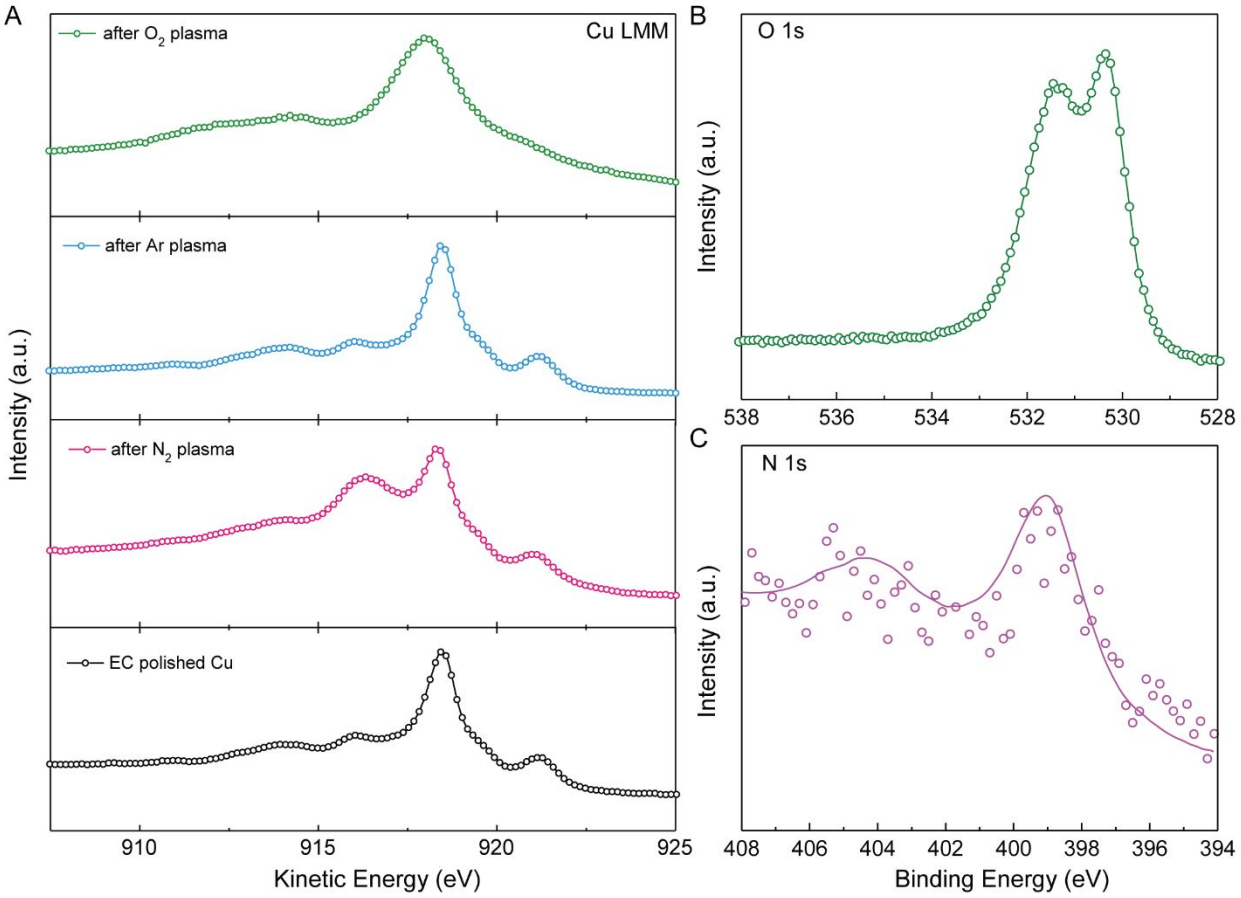

Figure S4. High-resolution core level XPS characterization. (A) Cu LMM spectra recorded on the foil electrodes after different plasma treatments. Both EC polished Cu and Ar plasma treated Cu foils exhibit a major feature of metallic Cu(0) peak at ~918.5 eV, while a broad shoulder peak located at 915.3~917.6 eV is observed for N_2 plasma treated Cu possibly arisen from the overlapped Cu(I) peak, and an oxidized surface feature consisting of Cu(I) and Cu(II) peaks is observed after O_2 plasma treatment (*Sur. Interface Anal.* 2017, *49*, 1325-1334), in accordance with the XPS and Raman spectra shown in Fig. 2. (B) O 1s and (C) N 1s spectra of 10-min O_2 and N_2 plasma pre-treated Cu foils, respectively.

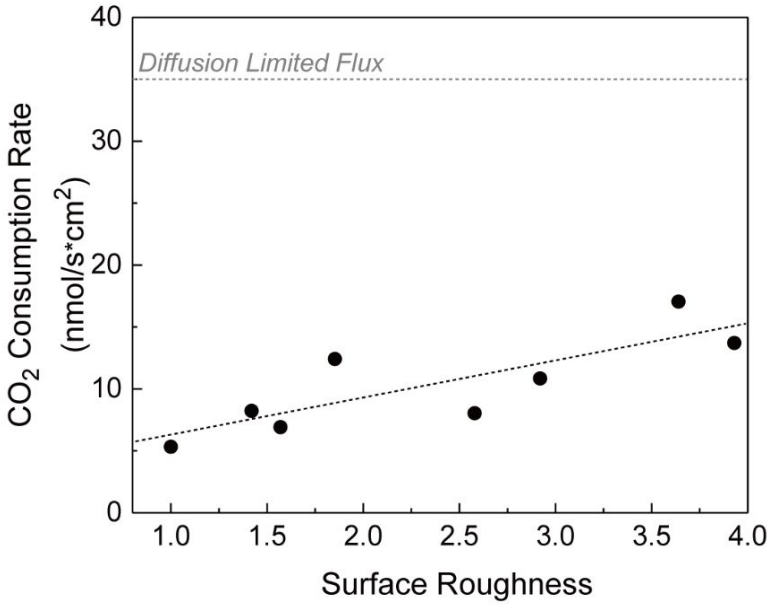

Figure S5. CO_2 consumption rate as a function of Cu surface roughness. The consumed CO_2 fluxes during chronoamperometric measurements at -1.0 V vs RHE are below CO_2 mass transport limitation of a planar electrode (as marked in grey line for reference).

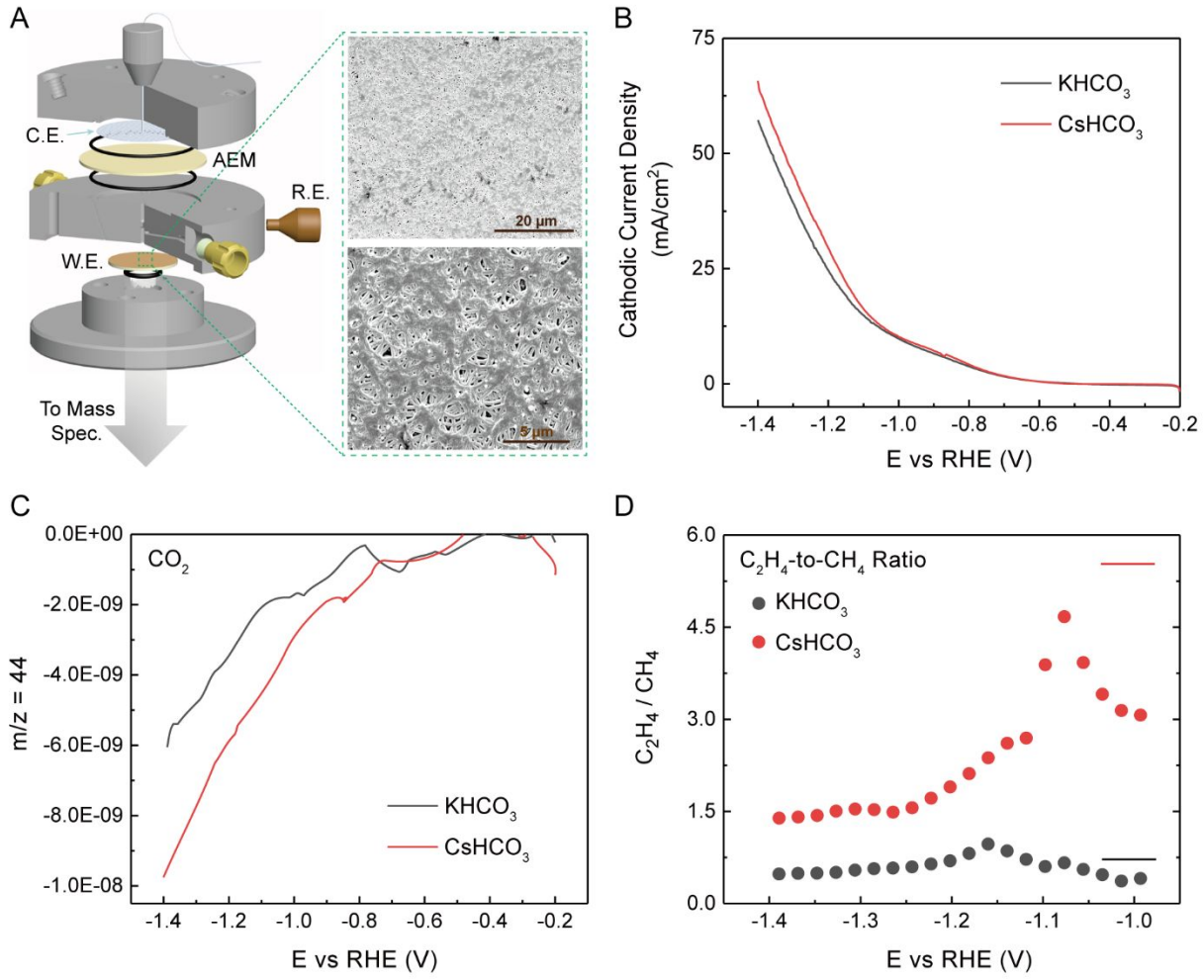

Figure S6. Cation effect investigation by DEMS. (A) Schematic of DEMS cell setup and representative SEM images of Cu film electrodes. (B) Geometric current density and (C) m/z=44 signals of CO_2 recorded during the negative potential sweep of 1 mV/s in CO_2-saturated 0.1 M $KHCO_3$ or $CsHCO_3$ electrolyte. (D) Observed C_2H_4/CH_4 ratio during the potential sweep, relevant m/z of 26 and 15 are recorded for each species, respectively. The solid lines represent the relative molar ratio of C_2H_4/CH_4 produced over polycrystalline Cu during chronoamperometry at −1 V vs RHE in a compact cell when analyzing the bulk electrolyte.

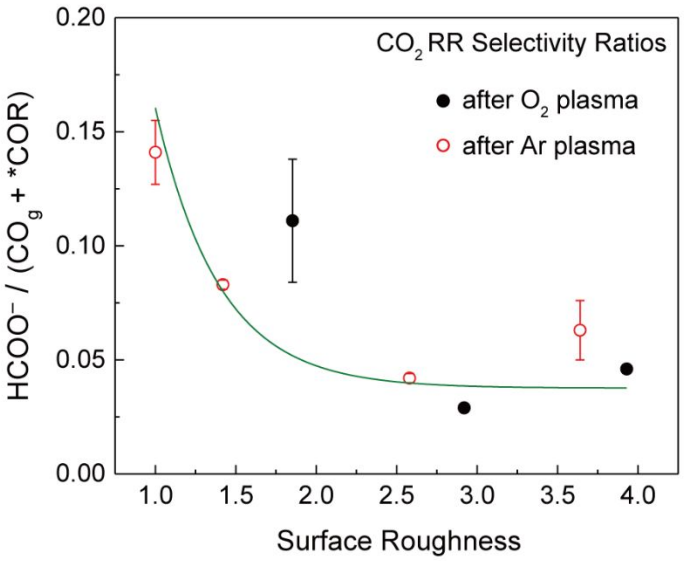

Figure S7. FE for formate relative to FE for CO_g and COR products as a function of Cu surface roughness.

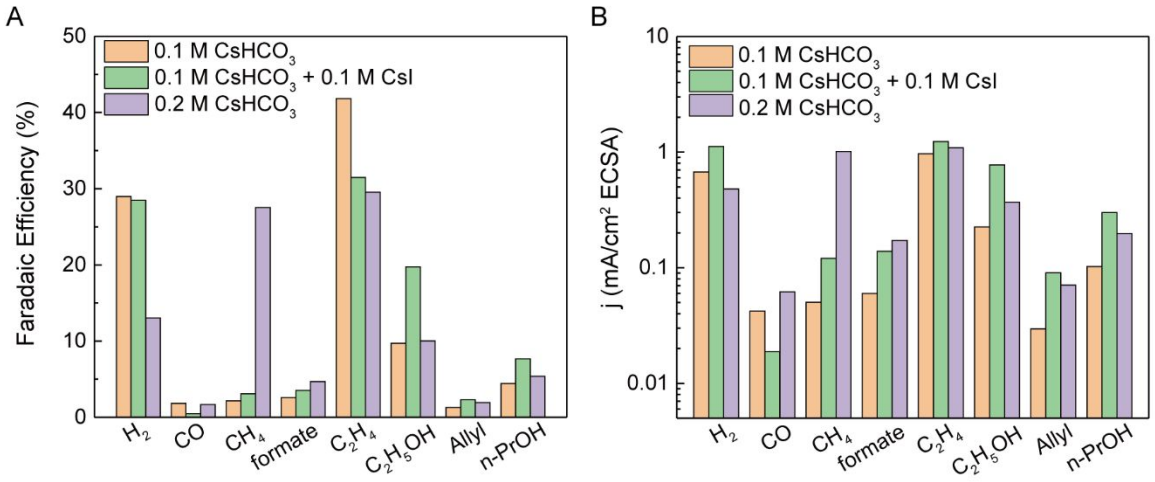

Figure S8. Control experiments of CO_2RR on 10-min Ar plasma pre-treated Cu foil electrodes within varied electrolyte composition. The determined relative surface roughness after 1-h electrolysis in 0.1 M $CsHCO_3$, 0.1 M $CsHCO_3$ + 0.1 M CsI and 0.2 M $CsHCO_3$ are ca. 2.6, 6.0 and 3.0, respectively. In agreement with Hori's early report on anion buffering effect (*Bull. Chem. Soc. Jpn.*, **1991**, *64*, 123-127), both the selectivity and activity of CH_4 evolution sharply increase after doubling HCO_3^- concentration, largely due to the suppression of local pH change during the electrolysis. On the other hand, the presence of I^- further increases Cu surface roughness, leading to the increased generation rate of alcohols (ethanol, allyl alcohol and n-propanol) and methane while at the expense of CO evolution selectivity and activity, demonstrating a stronger *CO binding strength.

Table S1. Summary of reported aqueous CO_2RR performances around -1.0 V (vs. RHE) over roughened Cu electrodes by different methods.

Entry	Catalyst	Surf. R.F.	j_{ECSA} (mA/cm^2)	H_2 FE (%)	C_{2+} FE (%)	C_{2+}/C_1 Ratio	C_{2+}/CH_4 Ratio	Electrolyte	Ref.
1	Ar_{10min}-plasma Cu	2.6	2.32	31.2	57.2	8.7	28.4	0.1 M $CsHCO_3$	This Work
2	$O_{2,\ 10min}$-plasma Cu	2.9	2.91	32.8	58.8	9.3	20.7		
3	EC polished Cu	1	2.71	36.3	30.9	1.1	8.1		
4	Under-coord. Cu(751)	1	3.06	24.7	47.5	2.0	3.6	0.1 M $KHCO_3$	*PNAS* **2017**, *114*, 5918
5	KF-cycled Cu foil	1.7	3.83	58	28	4.9	12.9	0.1 M $KHCO_3$	*ChemElectChem* **2016**, *3*, 1012
6	Cu dendrite on Cu foam	4.1	5.61	37	42	4.2	N.A.	0.5 M $NaHCO_3$	*ACS Catal.* **2016**, *6*, 3804
7	3.6-μm Cu_2O film	5.5	6.36	38.9	50.8	10.8	158	0.1 M $KHCO_3$	*ACS Catal.* **2015**, *5*, 2814
8	dendritic Cu on textured Si	7	1.29	38.3	47.9	4.4	48	0.1 M $CsHCO_3$	*Energy Environ. Sci.* **2019**, *12*, 1068
9	Cu_{vac}-on-Cu_2S	8.2	3.78	18.5	48.5	1.6	162	0.1 M $KHCO_3$	*Nat. Catal.* **2018**, *1*, 421
10	Cu-on-Cu_3N	9.7	1.84	17	63.7	7	25.5	0.1 M $KHCO_3$	*Nat. Commun.* **2018**, *9*, 3828
11	OD-$Cu_{3C,deposition}$	11	2.27	44	33	1.2	11	0.1 M $KHCO_3$	*PCCP* **2014**, *16*, 12194
12	$O_{2,\ 20W/2min}$-plasma Cu foil	26.4	1.06	50	32	10.7	16	0.1 M $KHCO_3$	*Nat. Commun.* **2016**, *7*, 12123
13	O_2-plasma Cu foil w/o I^-	26.6	1.92	30.5	69	19.7	46	0.1 M $CsHCO_3$	*ACS Catal.* **2018**, *8*, 10012
14	O_2-plasma Cu foil within CsI	38.7	1.70	40	69	41	138	0.1 M $CsHCO_3$ + 0.1 M CsI	
15	100-cycle Cu	41.9	1.61	21	60.5	2.7	4.7	0.25 M $KHCO_3$	*Nat. Catal.* **2018**, *1*, 111

Supporting References

1. Clark, E. L.; Resasco, J.; Landers, A.; Lin, J.; Chung, L.-T.; Walton, A.; Hahn, C.; Jaramillo, T. F.; Bell, A. T., Standards and Protocols for Data Acquisition and Reporting for Studies of the Electrochemical Reduction of Carbon Dioxide. *ACS Catal.* **2018,** *8* (7), 6560-6570.

2. McCrory, C. C. L.; Jung, S.; Peters, J. C.; Jaramillo, T. F., Benchmarking Heterogeneous Electrocatalysts for the Oxygen Evolution Reaction. *J. Am. Chem. Soc.* **2013,** *135* (45), 16977-16987.

3. Clark, E. L.; Ringe, S.; Tang, M.; Walton, A.; Hahn, C.; Jaramillo, T. F.; Chan, K.; Bell, A. T., Influence of Atomic Surface Structure on the Activity of Ag for the Electrochemical Reduction of CO_2 to CO. *ACS Catal.* **2019,** *9* (5), 4006-4014.

4. van Duin, A. C. T.; Dasgupta, S.; Lorant, F.; Goddard, W. A., ReaxFF: A Reactive Force Field for Hydrocarbons. *J. Phys. Chem. A* **2001,** *105* (41), 9396-9409.

5. Cheng, T.; Xiao, H.; Goddard, W. A., Nature of the Active Sites for CO Reduction on Copper Nanoparticles; Suggestions for Optimizing Performance. *J. Am. Chem. Soc.* **2017,** *139* (34), 11642-11645.

6. Huang, Y.; Chen, Y.; Cheng, T.; Wang, L.-W.; Goddard, W. A., Identification of the Selective Sites for Electrochemical Reduction of CO to C_{2+} Products on Copper Nanoparticles by Combining Reactive Force Fields, Density Functional Theory, and Machine Learning. *ACS Energy Lett.* **2018,** *3* (12), 2983-2988.

7. Chen, Y.; Huang, Y.; Cheng, T.; Goddard, W. A., Identifying Active Sites for CO_2 Reduction on Dealloyed Gold Surfaces by Combining Machine Learning with Multiscale Simulations. *J. Am. Chem. Soc.* **2019,** *141* (29), 11651-11657.

8. Huang, Y.; Kang, J.; Goddard, W. A.; Wang, L.-W., Density functional theory based neural network force fields from energy decompositions. *Phys. Rev. B* **2019,** *99* (6), 064103.